Supplementary information

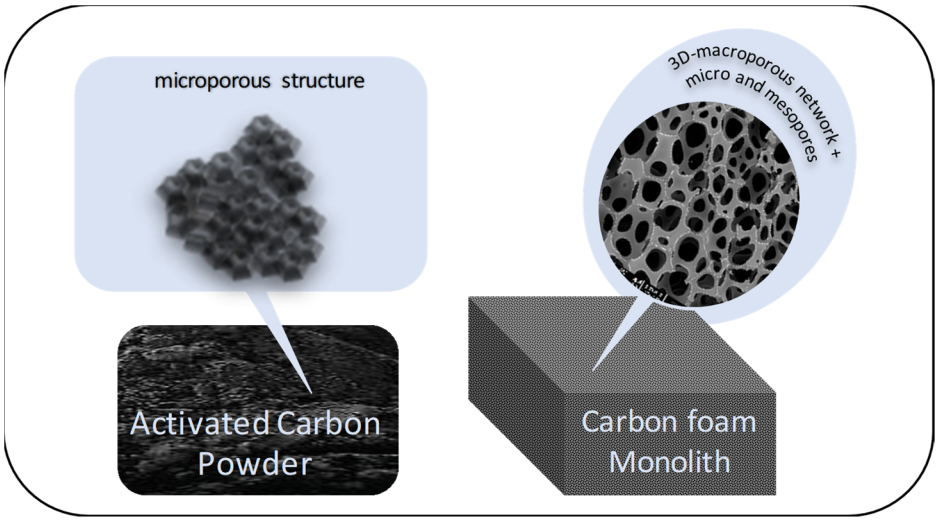

Figure S1. Structure of AC and SF highlighting the microporous and macroporous structure, respectively.

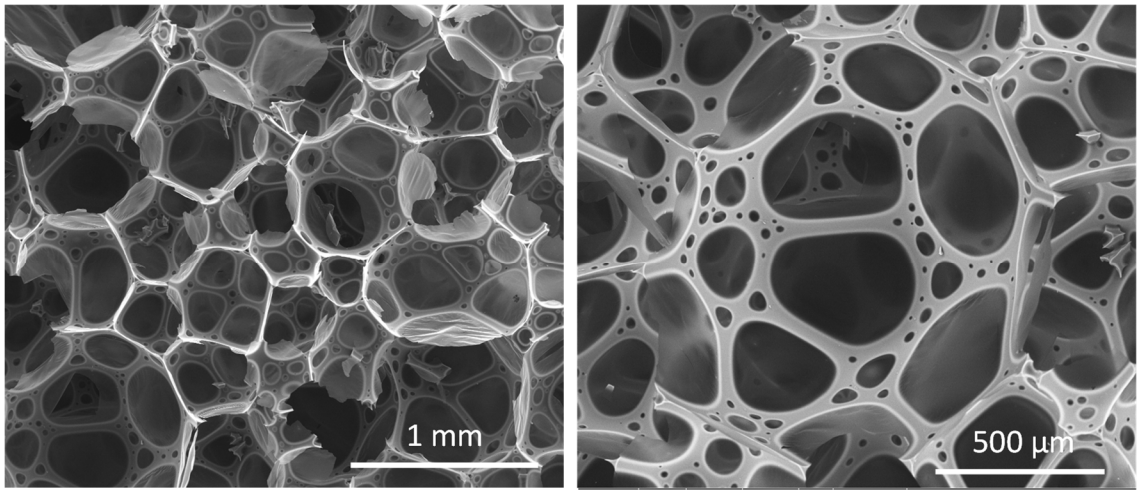

Figure S2. SEM images of SF.

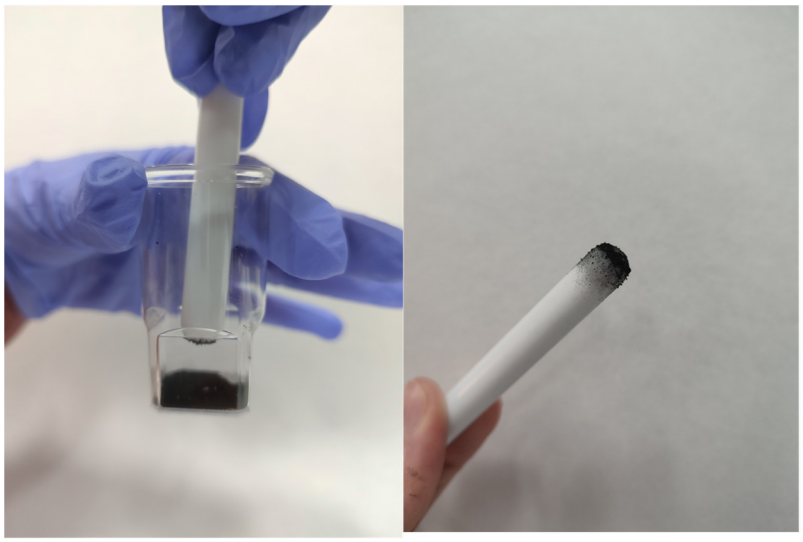

Figure S3. The magnetic property of ACFe-1.

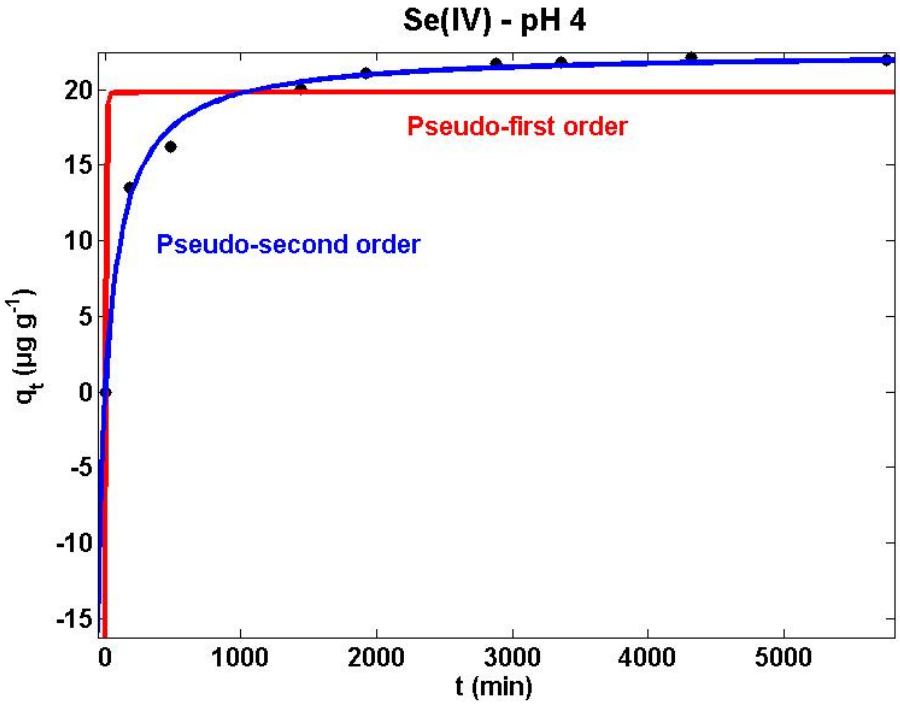

Figure S4. Removal of Se(IV) using ACFe-1 (initial concentration, 25 mg L^{-1}; 10 g L^{-1}; pH 4, 25 ºC). Correlation with pseudo-first order and pseudo-second order kinetic models.

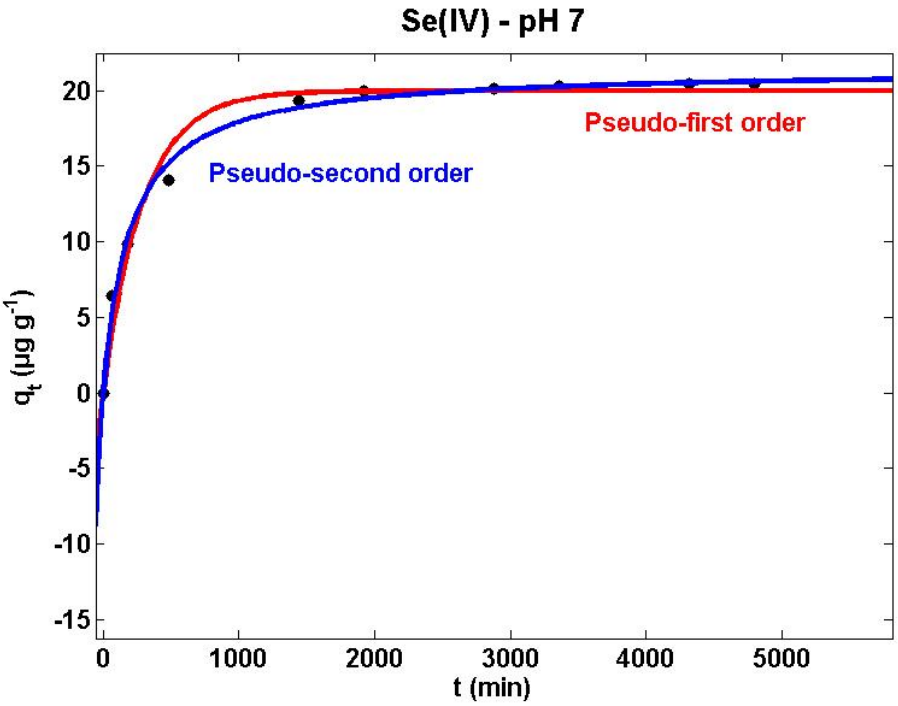

Figure S5. Removal of Se(IV) using ACFe-1 (initial concentration, 25 mg L^{-1}; 10 g L^{-1}; pH 7, 25 ºC). Correlation with pseudo-first order and pseudo-second order kinetic models.

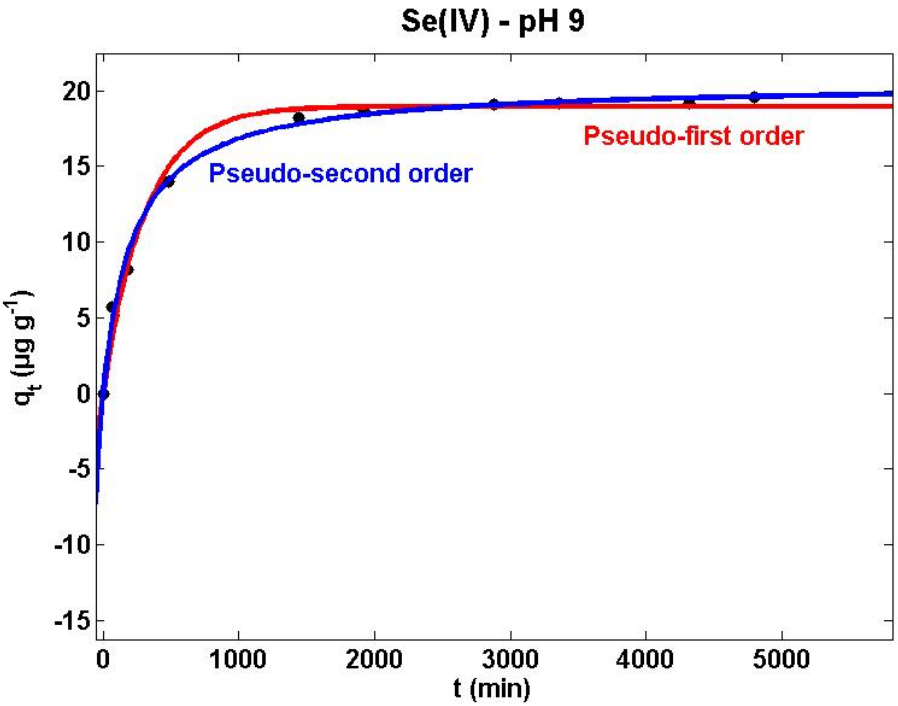

Figure S6. Removal of Se(IV) using ACFe-1 (initial concentration, 25 mg L^{-1}; 10 g L^{-1}; pH 9, 25 ºC). Correlation with pseudo-first order and pseudo-second order kinetic models.

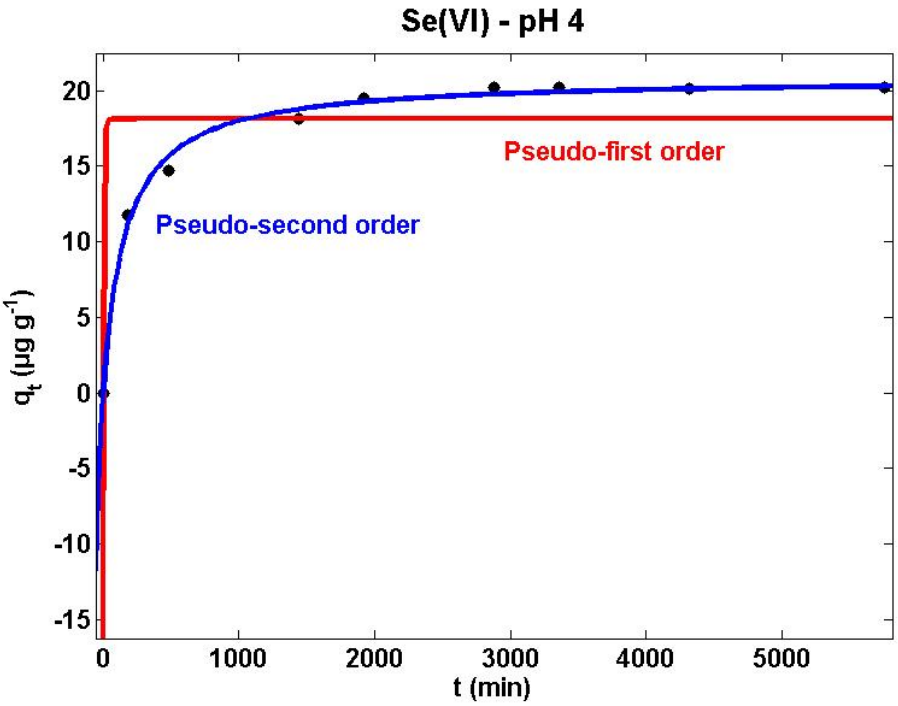

Figure S7. Removal of Se(VI) using ACFe-1 (initial concentration, 25 mg L^{-1}; 10 g L^{-1}; pH 4, 25 ºC). Correlation with pseudo-first order and pseudo-second order kinetic models.

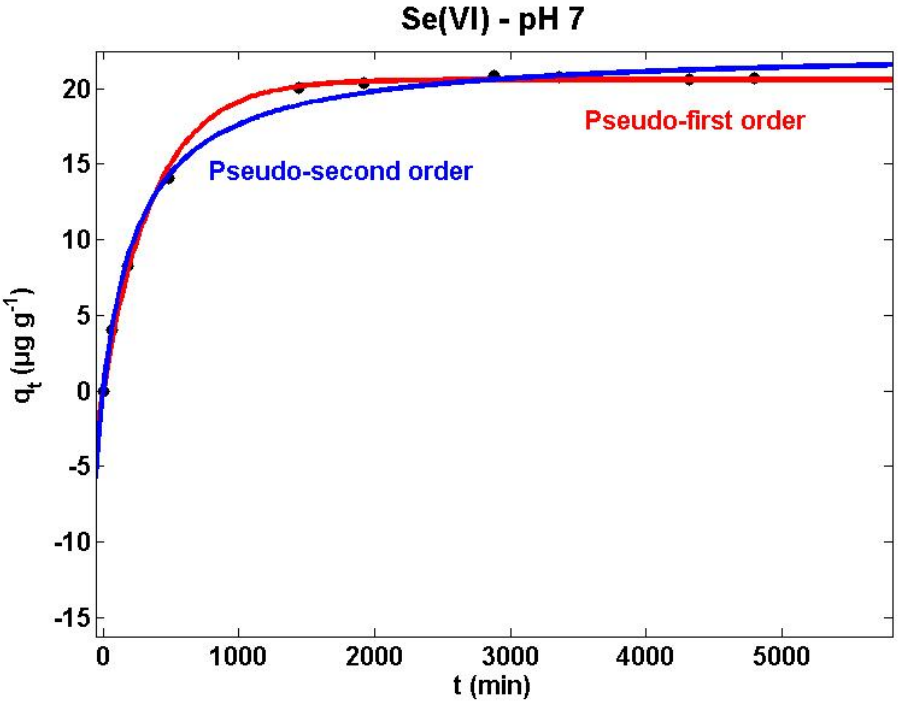

Figure S8. Removal of Se(VI) using ACFe-1 (initial concentration, 25 mg L^{-1}; 10 g L^{-1}; pH 7, 25 ºC). Correlation with pseudo-first order and pseudo-second order kinetic models.

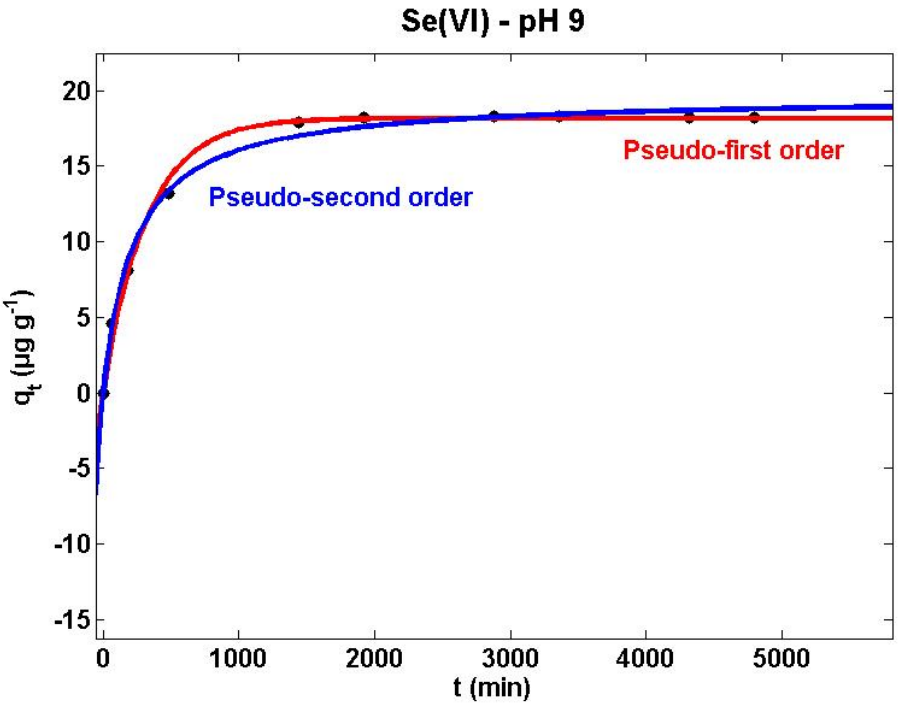

Figure S9. Removal of Se(VI) using ACFe-1 (initial concentration, 25 mg L^{-1}; 10 g L^{-1}; pH 9, 25 ºC). Correlation with pseudo-first order and pseudo-second order kinetic models.